Noise Considerations in Pulse-Shaping Based TIA Channel Designed for a Pulsed TOF Laser Radar Receiver

Aram Baharmast and Juha Kostamovaara
Circuits and Systems Research Unit (CAS)
ITEE Faculty, University of Oulu
Oulu, Finland
aram.baharmast@oulu.fi, juha.kostamovaara@oulu.fi

***Abstract*— In this study a detailed noise analysis and measurements of a time-of-flight (TOF) laser radar front-end amplifier are presented, in which an LC pulse shaper is combined with the non-linear feedback Trans-Impedance Amplifier in order to achieve a low noise and wide dynamic range TOF receiver. The noise of the receiver limits the single shot precision and sensitivity (i.e. the dynamic range at low end) of the receiver channel. It is shown that the proposed technique shapes the noise generated by various components of the front-end. Furthermore, in order to achieve the best possible noise performance, various compromises over different characteristics of the front-end (walk error, bandwidth) are discussed. The proposed front-end amplifier was fabricated as a part of a TOF receiver chip in a 0.35 µm standard CMOS process and our measurements show a trans-impedance gain of ~122 dBΩ, a bandwidth of ~200 MHz, and an input-referred equivalent current noise of ~60 nA.**

Keywords—time-of-flight (TOF), trans-impedance amplifier (TIA), pulse shaping technique, unipolar-to-bipolar conversion, noise analysis, dynamic range (DR), laser radar receiver

I. INTRODUCTION

The time-of-flight (TOF) measurement technique refers to the travel time of an optical pulse from a laser pulse transmitter to an observed object and back to the receiver. TOF based laser range finders are widely used in present industries (e.g. measurement of level heights in silos, positioning of tools and vehicles, and proximity sensors [1]). More recent applications include 3D scanning systems, which have application in robotics and automatic driving vehicles [2].

From a general point of view, optical receivers are part of both optical communications and TOF laser radar systems. In both the applications, an optical receiver resolves the value of the incoming signal by sensing the changes in the magnitude of the photodiode current [3, 4]. In optical communication receivers, the lowest possible noise and best possible sensitivity are achievable with input bandwidth far less than the bit rate frequency (e.g. 0.12 [5] to 0.6 f_{bit} [3]). However, an equalization technique is needed in order to eliminate inter-symbol interference (ISI) caused by adjacent symbols [6].

The optical TOF receivers, on the other hand, are not subject to ISI since the incoming pulses are spaced apart with sufficient time span (The maximum pulse rate in these systems is 100 KHz–1 MHz). In this type of receivers, however, the amplitude dependent timing error (known as walk error) and noise generated timing jitter dominantly limit the performance of the system [7–9]. The amount of jitter, which determines the single shot precision of the receiver channel, is directly proportional to the noise in the receiver channel and to the rise time of the arrived pulse [8]. The rise time, on the other hand, determines the bandwidth of the receiver channel. The maximum achievable bandwidth is determined using a specific technology; therefore, in order to increase the precision and sensitivity of the receiver channel, low noise solutions should be utilized.

An ongoing challenge in TOF receivers is that amplitude of the arrived echo pulse varies over a dynamic range (DR) of 1:10000 or even more depending on distance, weather condition, reflectivity and angle of the object. The receiver should be able to detect echo pulses in a range of less than 1 µA to more than 10 mA. If a simple comparator with a predefined threshold voltage is used to pick out the timing moment (known as leading edge detection method [10]) a large amount of walk error is produced (Fig. 1). To overcome this problem, one possible solution is the unipolar-to-bipolar conversion technique, in which the arrived unipolar pulse is converted to a bipolar signal and the first zero crossing point of the converted pulse is adopted as the timing point [11]. Using this technique is advantageous from both the DR and the walk error points of view because if the receiver channel is designed to recover fast from saturation in large input pulses, the zero crossing timing point remains unaffected. As a result, the DR of the receiver is enhanced while keeping the walk error low. An implementation of this technique is shown in Fig. 2, in which the input pulse passes through an RLC tank and generates a bipolar voltage signal, which is amplified by a differential amplifier. This implementation, however, suffers from excessive noise already generated at the input of the receiver channel due to relatively low damping resistor used in the RLC network.

In another implementation of this technique, which was recently proposed ([12, 13]), the LC resonator is combined with a non-linear shunt feedback TIA. This study undertakes

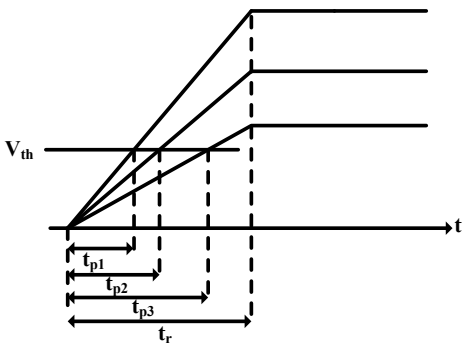

Fig. 1. Amplitude dependent timing error, known as walk error.

The authors acknowledge financial support from the Academy of Finland (Centre of Excellence in Laser Scanning Research, contract no. 307362) and the Infotech Oulu Graduate School.

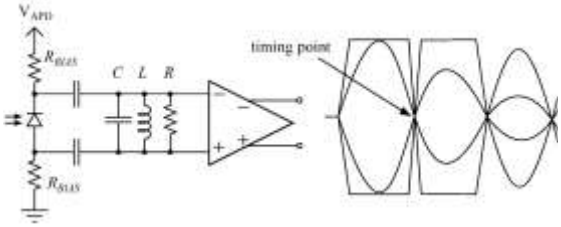

Fig. 2. Proposed circuit level implementation of the unipolar-to-bipolar conversion technique in [11].

a detailed analysis and measurements of the noise performance for this technique. The designed receiver based on this technique provides a low noise and a wide DR while keeping the walk error low without using complicated calibration methods. The rest of the paper is organized as follows: The effect of noise in TOF receivers is discussed in section II; after a short introduction to the proposed technique in section III, its noise performance is analyzed in section IV and V. Finally, the measured results and conclusions are presented in sections VI and VII respectively.

II. General Considerations

It has been long understood that in a bandwidth limited communication system, for a given rise time of the arrived pulse, the required bandwidth is roughly determined using the following equation ([14]).

$$BW \approx 0.35/t_r \tag{1}$$

where, t_r is the rise time of the arrived pulse. It means that in order to process steeper pulses, a wider bandwidth is needed. Another important parameter in the TOF leading edge optical receivers, which limits the precision of the receiver randomly, is the timing jitter. Based on triangulation estimation for a pulse ([15]), the timing jitter can be approximated by the following.

$$\sigma_{jitter} \approx \frac{\sigma_{noise}}{\partial V/\partial t} = \frac{t_r}{SNR} \tag{2}$$

where σ_{jitter} is the standard deviation of the timing point, σ_{noise} is the noise power and $\partial V/\partial t$ is the slope of the signal at the timing point (Fig. 3). This equation reveals an initial conflict between low-noise requirement and high-speed operation. For processing steeper signals, a higher bandwidth is required, which roughly leads to a higher in-band noise and consequently increases the amount of jitter. Furthermore, the amount of noise at the input of the receiver limits its sensitivity or the DR at low end.

III. Operation Principle

A basic block diagram of the proposed unipolar-to-bipolar conversion technique is depicted in Fig. 4. In this technique, the detected current pulse of the avalanche photo-diode (APD) is converted to a bipolar current signal through the LC tank, which is fed to a TIA. The TIA converts the arrived current signal to an amplified voltage at its output. In this configuration, no bias or front-end resistors are used and the

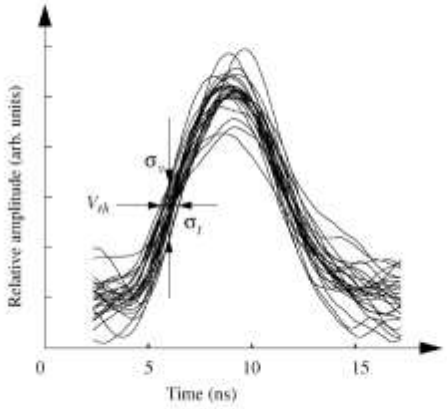

Fig. 3. The effect of noise in timing jitter.

under-damping response of the RLC network, which is needed in order to generate a bipolar signal, is set by the resistance seen at the input of the TIA, as given by the following expression.

$$R_{in,TIA} = \frac{R_F}{(A_0+1)} \tag{3}$$

where R_F is the feedback resistor and A_0 is the gain of the core amplifier (A). Therefore, if enough gain is provided a large feedback resistor can be chosen. Furthermore, the off-chip inductor (L) serves as part of the pulse-shaping unit and part of the APD bias circuitry. The commercially available inductors with high quality factor (e.g. 50) and low DC resistance (e.g. 2–5 Ω) fit our target frequencies (below 300 MHz) well.

In addition to the damping demands, the design criteria for this front-end arise from required bandwidth, minimization of noise and walk error. The bandwidth of the receiver channel is specified by the dominant pole of the TIA as [12, 16] given below.

$$\omega_{-3\mathrm{dB}} \cong \frac{A_0+1}{2R_FC_T} + \sqrt{\frac{1}{LC_T} + \left(\frac{A_0+1}{2R_FC_T}\right)^2} \tag{4}$$

where C_T is the total input node capacitance which includes the photodiode and the parasitic capacitance of the input pad and bonding wires. The value of this capacitance critically affects the performance of the system in terms of the noise level and walk error.

IV. Noise Analysis of the Proposed front-end

The Noise sources of the proposed front-end are shown in Fig. 4b. Based on [17] and neglecting the input current noise of the core amplifier, the equivalent noise at the input of the trans-impedance amplifier is:

$$\overline{I_{n,in}^2} = |H_1(s)|^2\overline{V_{n,RF}^2} + |H_2(s)|^2\overline{V_{n,A}^2} \tag{5}$$

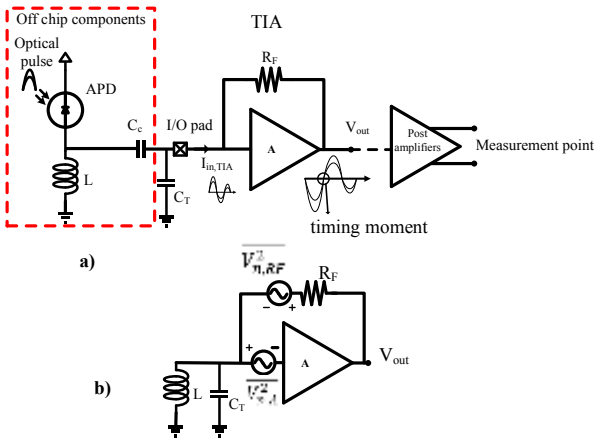

Fig. 4. A block diagram for the proposed front-end (a) and its equivalent noise model (b).

where $\overline{V_{n,RF}^2}$ is the noise voltage of the feedback resistor, $\overline{V_{n,A}^2}$ is the input referred voltage noise of the core amplifier, and

$$H_1(s) = \frac{1}{R_F} \times \frac{\frac{A_0}{R_F C_T} s}{s^2 + \frac{(1+A_0)}{R_F C_T} s + \frac{1}{LC_T}} \tag{6}$$

$$H_2(s) = \frac{A_0}{R_F} \times \frac{s^2 + \frac{1}{R_F C_T} s + \frac{1}{LC_T}}{s^2 + \frac{(1+A_0)}{R_F C_T} s + \frac{1}{LC_T}} \tag{7}$$

$H_1(s)$ and $H_2(s)$ are the input referred noise transfer functions of the feedback resistor and the core amplifier, respectively. $H_1(s)$ has a second order band-pass nature, while $H_2(s)$ has a second order band-stop nature. Fig. 5 shows the frequency response of these two transfer functions for a typical set of parameters. Based on this analysis, the noise generated by the feedback resistor manifests itself around the resonance frequency of the LC pulse-shaping circuit and is filtered out in other frequencies while the noise components of the core amplifier are filtered out in the vicinity of the resonance frequency. This "noise shaping" is a result of utilizing the proposed unipolar-to-bipolar conversion technique. The reason for this behavior is that at low frequencies, the inductor (L) and at high frequencies the capacitor (C_T) provide a low impedance pass to the ground and allow the noise of the core amplifier to be amplified by A_0, while bypassing the current noise of the feedback resistor to the ground. The bandwidth of these band-pass and notch transfer functions is roughly equal to

$$\mathrm{BW}_{Noise} \approx \frac{A_0}{2\pi R_F C_T} \tag{8}$$

This equation and analysis show a tradeoff between low noise requirements, bandwidth, trans-impedance gain and required damping for minimum walk error. More details about the noise considerations are given in the next section.

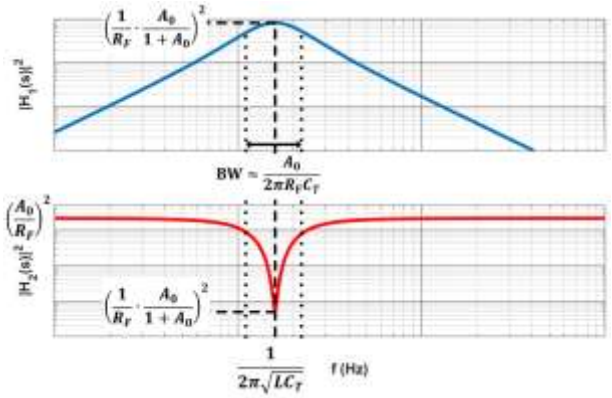

Fig. 5. The Frequency response of the input referred noise transfer functions ($H_1(s)$ and $H_2(s)$).

V. Noise Analysis of the Core Amplifier

The circuit level realization of the TIA is shown in Fig. 6a. The core amplifier (A) consists of two gain paths and a buffer: A1: a boosted cascode stage (M1, M2, MP1 and RL), A2: a common source stage (M4, M3) and Buff: a source follower stage (M5, M6). The output of the two gain paths is combined in a feedforward manner; however, A1 is the main gain stage and provides almost all the targeted gain. The common source stage has a gain of around one and due to that, it saturates at higher input amplitudes and returns to the linear region prior to the cascode stage. This feature eases recovery from saturation at large inputs and consequently minimizes the

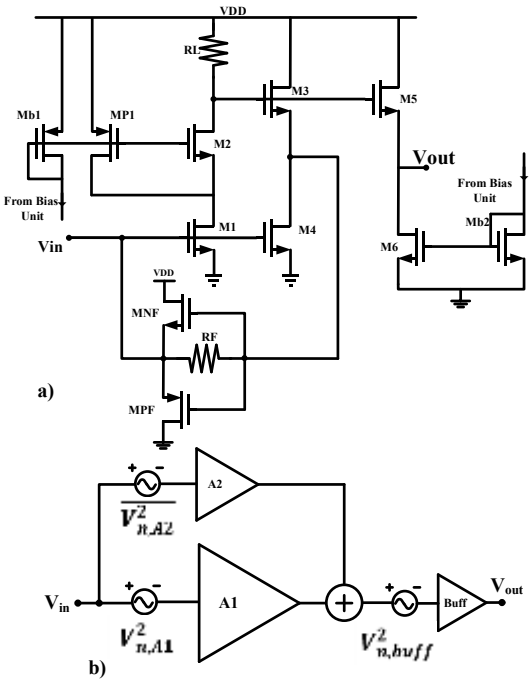

Fig. 6. Circuit level realization of the TIA and a simplified model for the noise sources of the core amplifier.

effect of saturation on the zero crossing point. A simplified model of the core amplifier along with the noise sources for each stage is shown in Fig. 6b. Based on this model the total input referred noise can be calculated as given below.

$$\overline{V_{n,A}^2} = \frac{A_1^2\overline{V_{n,A1}^2}+A_2^2\overline{V_{n,A2}^2}+\overline{V_{n,buff}^2}}{(A_1+A_2)^2} \approx \overline{V_{n,A1}^2} + \left(\frac{A_2}{A_1}\right)^2 \overline{V_{n,A2}^2} \quad (9)$$

where: $A_1 = g_{m1}R_L$, $A_2 = g_{m4}/g_{m3}$, and

$$\overline{V_{n,A1}^2} = 4KT\left(\frac{\gamma}{g_{m1}} + \frac{\gamma g_{mP1}}{g_{m1}^2} + \frac{1}{g_{m1}^2 R_L}\right) \quad (10)$$

$$\overline{V_{n,A2}^2} = 4KT\gamma\left(\frac{1}{g_{m4}} + \frac{g_{m3}}{g_{m4}^2}\right) \quad (11)$$

$$\overline{V_{n,\text{buff}}^2} = \frac{4KT\gamma}{g_{m5}^2}(g_{m5} + g_{m6}) \quad (12)$$

where all the variables represent their common meanings and the noise of the buffer is neglected in (9).

Based on this analysis, A1 contributes the most to the noise of the core amplifier. Therefore, based on (9), (6), and (7) in order to have the best possible noise performance, the following considerations should be taken into account:

1. The noise of the feedback resistor is filtered out both in high and low frequencies. Moreover, R_F appears in the denominator of both the noise transfer functions, therefore, its value should be chosen as large as possible, taking into account the bandwidth and damping required.

2. The gain of the core amplifier ($A_0 \approx A_1 = g_{m1}R_L$) appears in the numerator of its noise transfer function ($H_2(s)$), while g_{m1} is the most important parameter to alleviate the input referred noise of the core amplifier ($\overline{V_{n,A}^2}$); therefore, a good strategy would be to choose larger g_{m1} and smaller R_L. The contribution of R_L to the noise of the core amplifier is negligible; however, it can set the gain to be lower. It is important to note that A_0 affects the bandwidth of the signal and noise by the same rate ((8) and (4)) as well as input damping (3).

3. The thus far analysis for the noise of the front-end is based on infinite bandwidth for the core amplifier, and as a result, the noise generated by it does not experience any roll off at higher frequencies. Assuming a more realistic model for the core amplifier with single pole (which in our case is located at the drain of M2) leads to more complicated third order transfer functions for $H_1(s)$ and $H_2(s)$. This pole rolls off the noise generated from both feedback resistor and amplifier itself. The effect of this pole on $H_1(s)$ and $H_2(s)$ is shown in Fig. 7. From this figure, one may conclude that for a better noise performance a lower pole frequency would be advantageous. This is true but considering the frequency response of the whole trans-impedance amplifier channel, for having a maximally flat frequency response, the frequency of this pole should be at least two times the open-loop unity gain bandwidth of the front-end ([12], [16]). Furthermore, walk error related considerations for this front-end, which needs to be fast enough at large input pulse amplitudes to recover from saturation, does not allow the pole to be too close to the mentioned limit. Choosing smaller R_L is in line with these

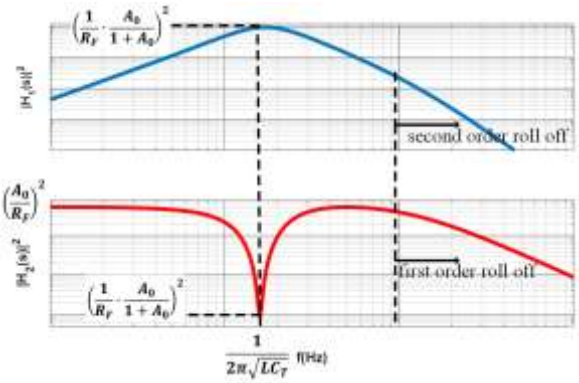

Fig. 7. Effect of the band limited core amplifier on the noise performance of the TIA.

demands. In addition, multiple roll offs will occur for high frequency noise as it passes through band-limited post amplifiers.

The proposed nonlinear feedback path preserves the damping resistance seen at the input of the TIA at large inputs and hence extends the DR of the receiver. The added transistors MNF and MPF are turned off for the small input currents. Therefore, they have no effect on the noise performance of the front-end. As the voltage drop across the feedback resistor increases, the transistors gradually turn on and steer the extra current from VDD to the input node (MNF) or from the input node to the ground (MPF). Without these two transistors, the output signal of the TIA would tend to oscillate at large inputs due to lack of sufficient damping [12].

VI. Measurement Results

The proposed technique was used to design a TOF receiver channel in a 0.35 µm standard CMOS technology. The die microphotograph of the TIA front-end is shown in Fig. 8. The values of R_F, L, g_{m1} and R_L are 5 KΩ, 250 nH, 26 ms, and 860 Ω, respectively (based on simulation). The total input capacitance based on measurements is ~4 pF. The front-end draws ~9 mA current from a single 3.3 V supply voltage. The

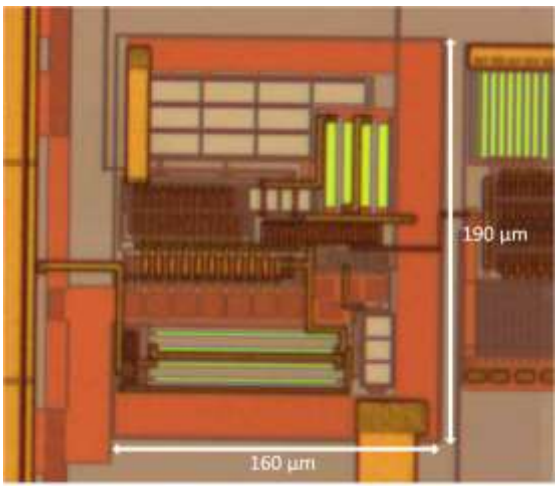

Fig. 8. The microphotograph of the fabricated TIA front-end.

total measured AC trans-impedance gain at the output of analog buffer is ~122 dBΩ, and the measured bandwidth is about 200 MHz (The output signal of the TIA is measured after it is further amplified by several gain stages). Fig. 9 shows the time domain analog output for an electrical input excitation. As can be seen, the unipolar input current pulse is perfectly converted to an amplified bipolar voltage through the channel. The total measured noise at the output of the analog buffer is 70 mV, or ~60 nA RMS when referred to the input. The measured output noise is shown in Fig. 10, where the FFT of the noise is also shown. A brief comparison between the proposed technique and state-of-the-art solutions is presented in Table I.

VII. Conclusion

In this paper, the noise performance of the previously proposed pulse-shaping based TIA front-end has been analyzed and various compromises on different parameters of the front-end have been discussed. It has been shown that this technique filters out the noise of the feedback resistor in both low and high frequency regions. Furthermore, to achieve the best possible noise performance, the values of R_F and g_{m1} (trans-conductance of the input transistor) should be high and R_L (the load resistance of the core amplifier input stage) should be low, taking into account the bandwidth demands too. The noise related measurements of the front-end have also been presented. The designed front-end holds an RMS input referred noise of ~60 nA. The whole receiver channel was designed and fabricated in a 0.35 µm standard CMOS process to be used in a wide DR TOF range finding system.

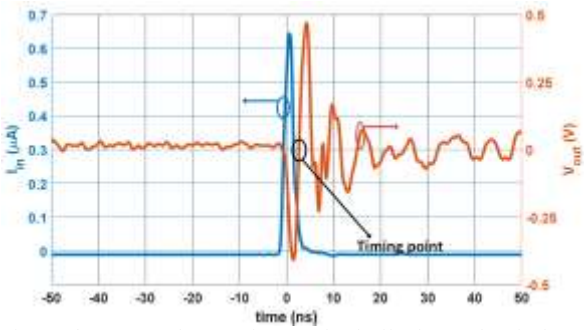

Fig. 9. The measured output from analog buffer for an electrical input excitation. The rise time of the input pulse is ~1.5 ns.

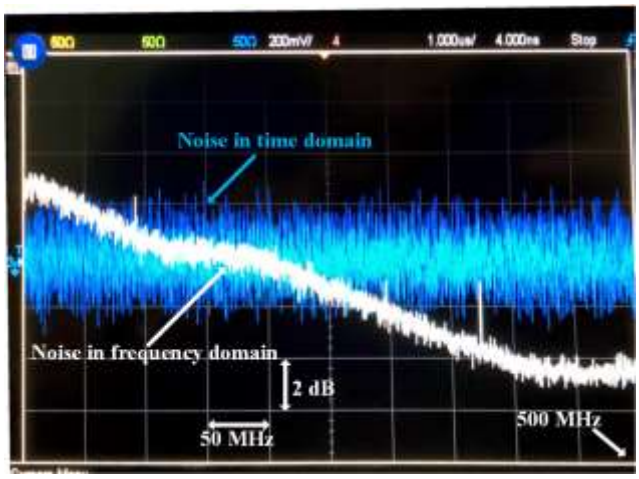

Fig. 10. The measured output noise along with its FFT.

TABLE I. SUMMARY OF MEASURED PARAMETERS AND COMPARISON WITH RECENTLY REPORTED FRONT-ENDS.

Specification	This work	[2]	[18]
Process	0.35µm standard CMOS	0.35µm standard CMOS	0.35µm standard CMOS
Supply voltage (V)	3.3	3.3	3.3
Power consumption of the front-end (mW)	30	NA	NA
Measured Bandwidth (MHz)	200	230	140
Trans-impedance gain (dBΩ)	122	NA	NA
Input referred noise current (nA)	60	100	19
Technique used in the front-end	TIA pulse shaping	differential TIA	Capacitor TIA (C-TIA)

References

[1] T. Ruotsalainen, P. Palojarvi, and J. Kostamovaara, "A wide dynamic range receiver channel for a pulsed time-of-flight laser radar," *IEEE Journal of Solid-State Circuits,* vol. 36, no. 8, pp. 1228-1238, 2001.

[2] S. Kurtti, J. Nissinen, and J. Kostamovaara, "A wide dynamic range CMOS laser radar receiver with a time-domain walk error compensation scheme," *IEEE Transactions on Circuits and Systems I: Regular Papers,* vol. 64, no. 3, pp. 550-561, 2017.

[3] M. H. Nazari and A. Emami-Neyestanak, "A 24-Gb/s double-sampling receiver for ultra-low-power optical communication," *IEEE Journal of Solid-State Circuits,* vol. 48, no. 2, pp. 344-357, 2013.

[4] S. Donati, *Electro-optical instrumentation: sensing and measuring with lasers*. Pearson Education, 2004.

[5] A. Sharif-Bakhtiar and A. C. Carusone, "A 20 Gb/s CMOS optical receiver with limited-bandwidth front end and local feedback IIR-DFE," *IEEE Journal of Solid-State Circuits,* vol. 51, no. 11, pp. 2679-2689, 2016.

[6] S. D. Personick, "Receiver design for digital fiber optic communication systems, I," *Bell system technical journal,* vol. 52, no. 6, pp. 843-874, 1973.

[7] P. Palojarvi, K. Maatta, and J. Kostamovaara, "Pulsed time-of-flight laser radar module with millimeter-level accuracy using full custom receiver and TDC ASICs," *IEEE Transactions on Instrumentation and Measurement,* vol. 51, no. 5, pp. 1102-1108, 2002.

[8] R. J. Van De Plassche and P. Baltus, "An 8-bit 100-MHz full-Nyquist analog-to-digital converter," *IEEE Journal of Solid-State Circuits,* vol. 23, no. 6, pp. 1334-1344, 1988.

[9] P. Palojarvi, T. Ruotsalainen, and J. Kostamovaara, "A 250-MHz BiCMOS receiver channel with leading edge timing discriminator for a pulsed time-of-flight laser

rangefinder," *IEEE Journal of solid-state circuits,* vol. 40, no. 6, pp. 1341-1349, 2005.

[10] S. Kurtti and J. Kostamovaara, "An integrated laser radar receiver channel utilizing a time-domain walk error compensation scheme," *IEEE Transactions on instrumentation and measurement,* vol. 60, no. 1, pp. 146-157, 2011.

[11] J. Pehkonen, P. Palojarvi, and J. Kostamovaara, "Receiver channel with resonance-based timing detection for a laser range finder," *IEEE Transactions on Circuits and Systems I: Regular Papers,* vol. 53, no. 3, pp. 569-577, 2006.

[12] A. Baharmast and J. Kostamovaara, "A low noise front end trans-impedance amplifier channel for a pulsed time-of-flight laser radar," in *Ph. D. Research in Microelectronics and Electronics (PRIME), 2017 13th Conference on*, 2017, pp. 285-288: IEEE.

[13] A. Baharmast, T. Ruotsalainen, and J. Kostamovaara, "A Low Noise, Wide Dynamic Range TOF Laser Radar Receiver Based on Pulse Shaping Techniques," in *Circuits and Systems (ISCAS), 2018 IEEE International Symposium on*, 2018, pp. 1-5: IEEE.

[14] R. Ziemer and W. H. Tranter, *Principles of communications: system modulation and noise*. John Wiley & Sons, 2006.

[15] G. Bertolini and A. Coche, *SEMICONDUCTOR DETECTORS*. Amsterdam, The Netherlands: North-Holland, 1968.

[16] E. Säckinger, *Broadband circuits for optical fiber communication*. John Wiley & Sons, 2005.

[17] B. Razavi, *Design of integrated circuits for optical communications*. John Wiley & Sons, 2012.

[18] H.-S. Cho, C.-H. Kim, and S.-G. Lee, "A high-sensitivity and low-walk error LADAR receiver for military application," *IEEE Transactions on Circuits and Systems I: Regular Papers,* vol. 61, no. 10, pp. 3007-3015, 2014.